16th World Conference on Earthquake Engineering, 16WCEE 2017

Santiago Chile, January 9th to 13th 2017

Paper N° 4937

Registration Code: S-11464476619

SEISMIC RESPONSE OF THE BASIN OF QUITO FROM CONTINUOUS ACCELEROMETRIC RECORDS OF RENAC-QUITO

A. Laurendeau[(1)], L-F. Bonilla[(2)], D. Mercerat[(3)], F. Courboulex[(4)], A. Alvarado[(5)], J. C. Singaucho[(6)], C. Viracucha[(7)], P. Guéguen[(8)], E. Bertrand[(9)]

(1) PhD, Instituto Geofísico Escuela Politécnica Nacional, Quito, Ecuador, alaurendeau@igepn.edu.ec
(2) Researcher, Université Paris Est, Institute of Science and Technology for Transport, Development and Networks (IFSTTAR), Marne la Vallée, France, fabian.bonilla@ifsttar.fr
(3) Researcher, CEREMA - Centre d'études et d'expertise sur les risques, l'environnement, la mobilité et l'aménagement, Nice, France diego.mercerat@cerema.fr
(4) Researcher, Université Nice Sophia Antipolis, CNRS, Observatoire de la Côte d'Azur, Géoazur, Valbonne, France, courboulex@geoazur.unice.fr
(5) Researcher, Instituto Geofisico Escuela Politecnica Nacional, Quito, Ecuador, aalvarado@igepn.edu.ec
(6) MSc, Instituto Geofísico Escuela Politécnica Nacional, Quito, Ecuador, jcsingaucho@igepn.edu.ec
(7) Laboratory worker, Instituto Geofisico Escuela Politecnica Nacional, Quito, Ecuador, aalvarado@igepn.edu.ec
(8) Researcher, University of Grenoble Alpes, ISTerre, F-38041 Grenoble, France, philippe.gueguen@univ-grenoble-alpes.fr
(9) Researcher, CEREMA - Centre d'études et d'expertise sur les risques, l'environnement, la mobilité et l'aménagement, Nice, France, Etienne.Bertrand@cerema.fr

Abstract

The city of Quito has been damaged several times in the past by important earthquakes. The seismic hazard assessment is thus an important issue and especially, the site effect question. The Quito basin deep structure remains unknown and the potential impact of seismic waves has yet to be evaluated. The Red Nacional de Acelerógrafos (RENAC) that began in 2009 now offers a sufficient numbers of high quality data to improve the knowledge of the potential site effects.

In this study, the horizontal-to-vertical spectral ratio method (HVSR) is employed from noise and earthquake records to estimate the resonant frequency peaks. In addition, the ambient noise recorded by the accelerometers is analyzed by seismic interferometry techniques. This study shows that the southern part of Quito has a behavior different than that of the northern part. The southern part amplifies especially around 0.3 Hz and also around 4 Hz. It's for example possible to observe longer duration and larger amplitude signals for this zone in the case of regional events. The observations suggest a possibly more pronounced site effect in the South due to thickening of the Quito basin in that direction.

Keywords: Ground motions – Quito basin site effects – HVSR – seismic interferometry – accelerometric records

1. Introduction

The city of Quito, capital of Ecuador, situated in a narrow Interandean depression (2200–3000 m in elevation) has been damaged several times by historical earthquakes (e.g., the 1859 event is the most destructive earthquake with Imax of VII-VIII) [1]. Built on the hanging wall of a very active thrust fault, with the population now approaching to 3 million inhabitants and much of its poorly constructed dwelling located on unstable sites, damage from future shaking in Quito could be devastating. The seismic hazard assessment is an important issue in Quito.

The Quito basin deep structure remains unknown and the potential impact of seismic waves has yet to be evaluated. Specifically, there is a lack of knowledge on the shape and extension of the basin, with respect to its depth, as well as the seismic velocities of the infilling material, which is mainly composed of volcanic ashes and magmatic intrusions. Several observations from previous studies indicate that this basin can greatly amplify seismic waves [2, 3]. Gueguen et al. (2000) [2] generally observed two distinct resonant frequencies for about 60 sites, particularly located in the central depression. In some cases, the second peak amplifies the surface ground motion more than the rest of the soil column. Alfonso-Naya et al. (2012) [3] observed low frequency amplification was associated with frequencies around 0.35 Hz in the South of Quito. However, these studies are based on only a few accelerometric records.

The Red Nacional de Acelerógrafos (RENAC) began in 2009 as part of the Secretaría de Educación Superior, Ciencia, Tecnología e Innovacción (SENESCYT) project. The first permanent accelerometers were installed in Quito during September 2009. Currently, 18 stations in free field deployment are sited on the Quito basin with continuous recording monitoring.

In this study, we utilize this valuable new database in several ways. First, the entire accelerometric database is used to estimate the horizontal-to-vertical spectral ratios (HVSR) [4, 5]. These spectral ratios are computed using automated routines. Second, the ambient noise recorded by the accelerometers is analyzed by seismic interferometry techniques.

2. Description of RENAC-QUITO

The RENAC of Quito was deployed since the end of 2009. It is now composed of 18 stations in proper working conditions with continuous recording of the soil acceleration at the free surface, and one station (CIVI), located at the top of a building (Fig. 1). Three stations are permanently shut down (COSF, IRDE, RUMP due to company relocations).

Each accelerometric station consists of a fully integrated triaxial accelerometer (Guralp CMG-5TD) and a 24-bit three-component digitizer (DM-24) sampling at 100 Hz. The instrumental response is flat from DC to 100 Hz. The full range of acceleration corresponds to 0.1 μG up to 4 g for all stations. Time is calibrated by a GPS receiver. The data are stored in GCF format on an internal 8 Gb flash memory. Each station is positioned on concrete slab floor inside a metal box at the free surface. For most stations, it is necessary to retrieve data on site, except for eight stations that telemeter direct information to the Instituto Geofísico de la Escuela Politécnica Nacional (IG-EPN) (BELL, CIVI, CRPG, EPNL, FENY, QUIB, SADP, VIFL) since the end of 2015.

The noise characteristics of each station are computed and compared with the accelerometric reference curves proposed by Cauzzi and Clinton (2013) [6] (Fig. 2). For all the stations, the noise level is included between the reference curves for frequencies less than 1 Hz. Around 1 Hz, the station-specific noise is close to the high reference model and even larger at frequencies higher than 25 Hz for the majority of stations. Thus, it is difficult to record the small and distant earthquakes without application of a highpass filter on the signal. Yet, this is expected for strong motion stations located in an urban area.

Fig. 3 displays the time-lines of each station. For most stations, these are not continuous but with a good rate of recording. Some stations as CUMB and ALLO present numerous gaps. In addition, a major part of the available data from IESS also has timing problems.

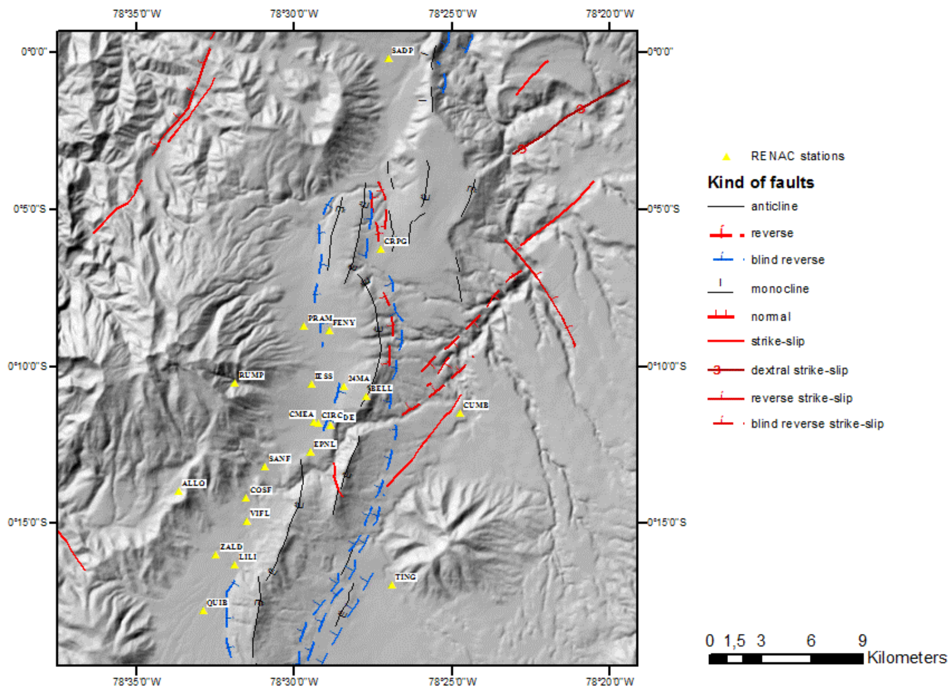

Fig. 1: Accelerometric stations of the RENAC network in Quito (yellow triangles) and active segments of faults (blue and red lines) identified by Alvarado et al. 2014 [7].

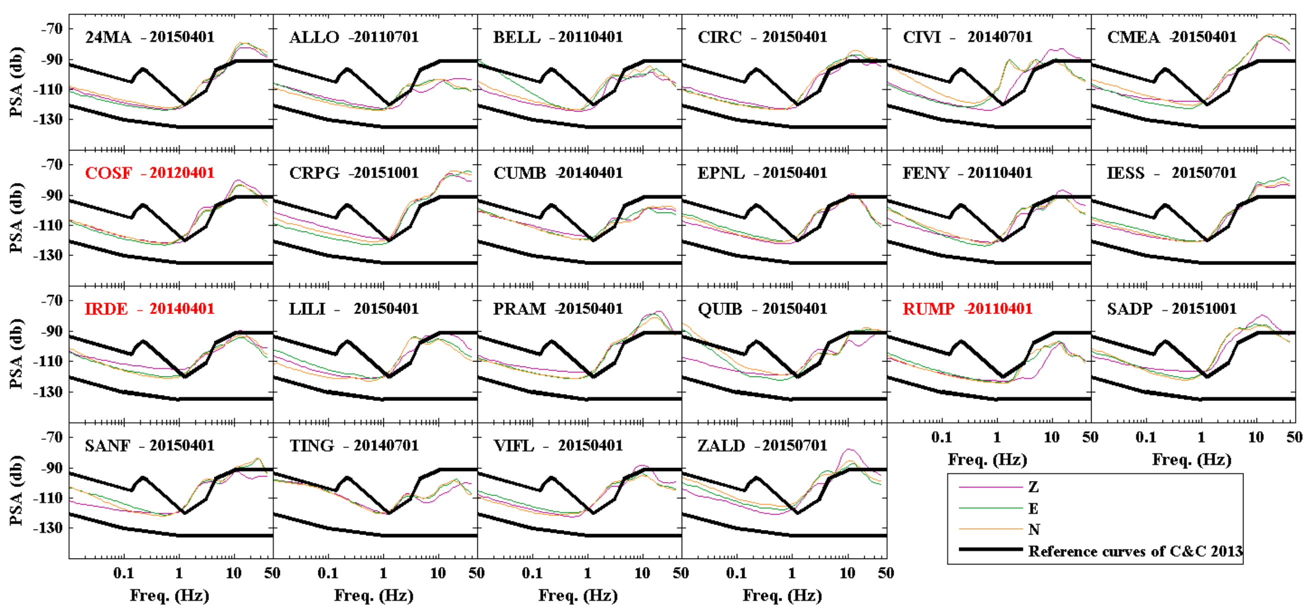

Fig. 2: Noise characteristics for accelerometric stations of RENAC. For each station, the power spectral amplitude is represented as the mean of 24 windows of one hour for each component. The noise characteri|stics are compared with the accelerometric high- (AHNM) and low- (ALNM) noise models of Cauzzi and Clinton (2013) [6] defined for high-quality accelerometers in the context of urban area.

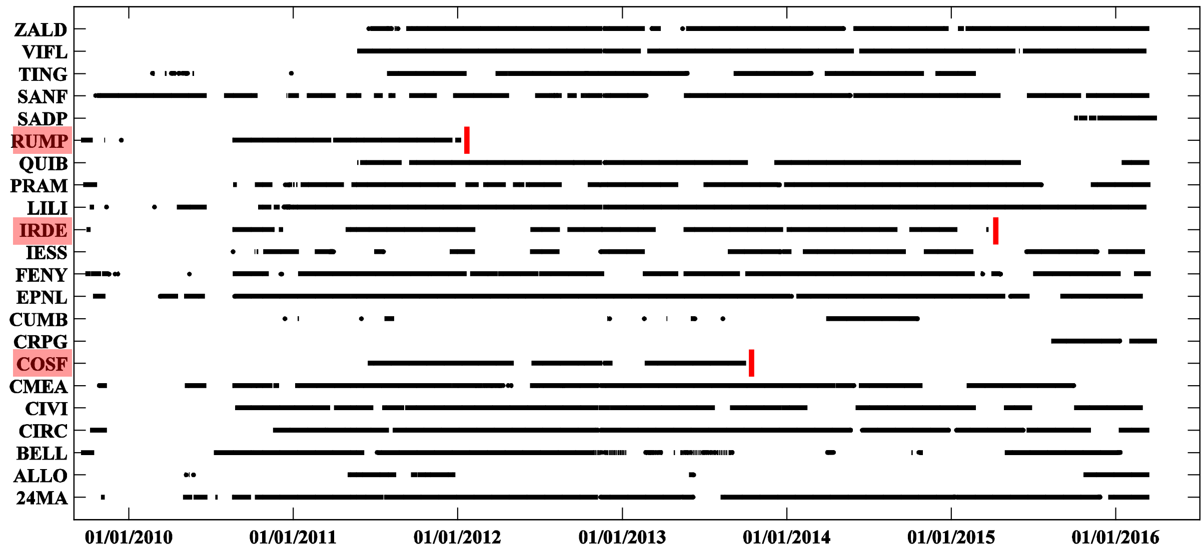

Fig. 3: Time-lines of the RENAC stations with the data available from the end of 2009 to 07/04/2016. The stations in red are permanently shut down.

3. The seismicity of Quito

The city of Quito is situated in a valley prone to seismic hazard. Many historical earthquakes have been reported such as the events of 1587, 1755, 1797, 1868 and 1949 that have produced intensities equal or larger than VII [8]. The last important earthquake that has strongly affected the city occurred in 1868 (Ibarra, maximum intensity IX, Mw 7.1 [1]). Quito can be strongly affected by three kind of earthquakes: (1) events with magnitude larger than 8.0 coming from the subduction zone located at more than 200 km (e.g., Esmeralda, 1906, Mw 8.8), (2) shallow events with a magnitude 7.0 to 7.5 from the Andes cordillera and originated about 80 km away or more and (3) events with a magnitude 6.0 to 7.0 occurring on faults close to the city.

The IGEPN monitors the instrumental seismicity of Ecuador with the Ecuadorian seismic network (The Red Nacional de Sismógrafos, RENSIG). The local catalog provides earthquake solutions for the time period 1990–present. Until May 2011, the reported magnitude is the duration magnitude (M_D) calculated on the coda waves from one record [9]. After May 2011, Seiscomp, a freely available software package developed at GFZ Potsdam [10, 11], is used. In the new catalog, the reported magnitude is a local magnitude (MLv) and it is a mean from different stations. Since October 2015, the 8 RENAC stations, which transmit direct information, are also used to determine the source locations and the magnitudes, especially for the major earthquakes. Beauval et al. (2013) [12] consider M_D to be a reasonable surrogate for M_W and we consider the same for MLv. 81 earthquakes of magnitude larger than 5 have been recorded by the national seismic network since the deployment of RENAC (Fig.4).

Fig. 5 displays the RENAC-QUITO records for a local event. This event occurred on August 12^{th} 2014 at 19h57m (UTM), and it was located in the north of the city, close to the locality of Calderón. It is an event of magnitude (MLv) 5.1, with a depth of 5.3 km and showing a reverse fault mechanism. For this earthquake, an intensity evaluation showed values of IV for most part of Quito, and for some districts close to the epicenter intensity up to VI [13]. This event allowed the observation of amplitude attenuation with the source distance. The nearest stations, FENY and PRAM, are located at 13 km with a maximum PGA of 38 cm/s^2 and 48 cm/s^2, respectively. After this event, two stations were deployed in the north of Quito (CRPG and SAPD), where near faults have been identified as potential sources of future events.

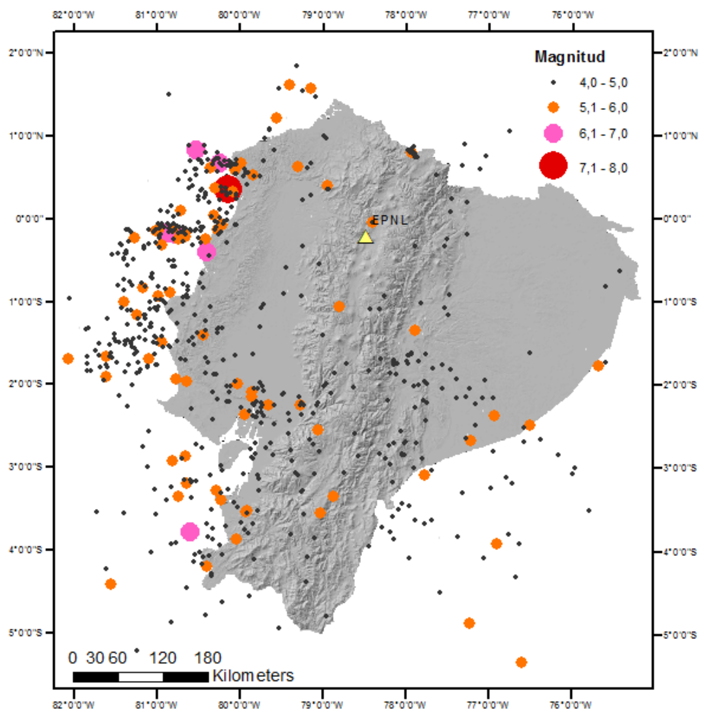

Fig. 4: Map of the major seismicity (magnitude larger than 4.0) recorded by the national seismic network since the deployment of RENAC, i.e. 01-10-2009 and until 30-04-2016. The location of the station EPNL is showed as a reference for Quito.

Fig. 6 presents a recent regional subduction event occurred on April 16th 2016 at 23:58 (UTM) close to Pedernales with Mw of 7.8 (USGS) and a depth of 17 km. This earthquake was located at the interface and results of the displacement of the Nazca tectonic plate (oceanic plate) that plunges under the South American plate (continental plate). This earthquake shares some similarities with the Mw 8.8 1906 Esmeralda earthquake. In Quito, it was felt with an intensity of IV-V [14]. In this context, the epicentral distance is approximatively the same for all the sites (around 170 km) and this allows highlighting possible site effects. On Fig. 6, it is possible to observe larger amplitude and duration for the sites localized in the South of Quito (VIFL, ZALD, LILI) and also in the north (SADP). On the contrary, the amplitude is smaller for stations in the center of Quito such as 24MA, CMEA, CIRC, EPNL. These observations suggest a possibly more pronounced site effect towards the south, due to thickening of the Quito basin in that direction.

4. Horizontal-to-vertical spectral ratio method (HVSR)

The horizontal-to-vertical-spectral-ratio (mHVSR) analysis method using ambient noise (microseism), as introduced by Nakamura (1989) [4], and the eHVSR using earthquake recordings, as introduced by Lermo and Chavez-Garcia (1993) [5], provide a means to estimate the fundamental resonance frequency (f_0) or the resonance frequencies, in presence of strong contrasts [15]. These methods, however, have been shown to not consistently retrieve the amplitude of the site response [16, 17].

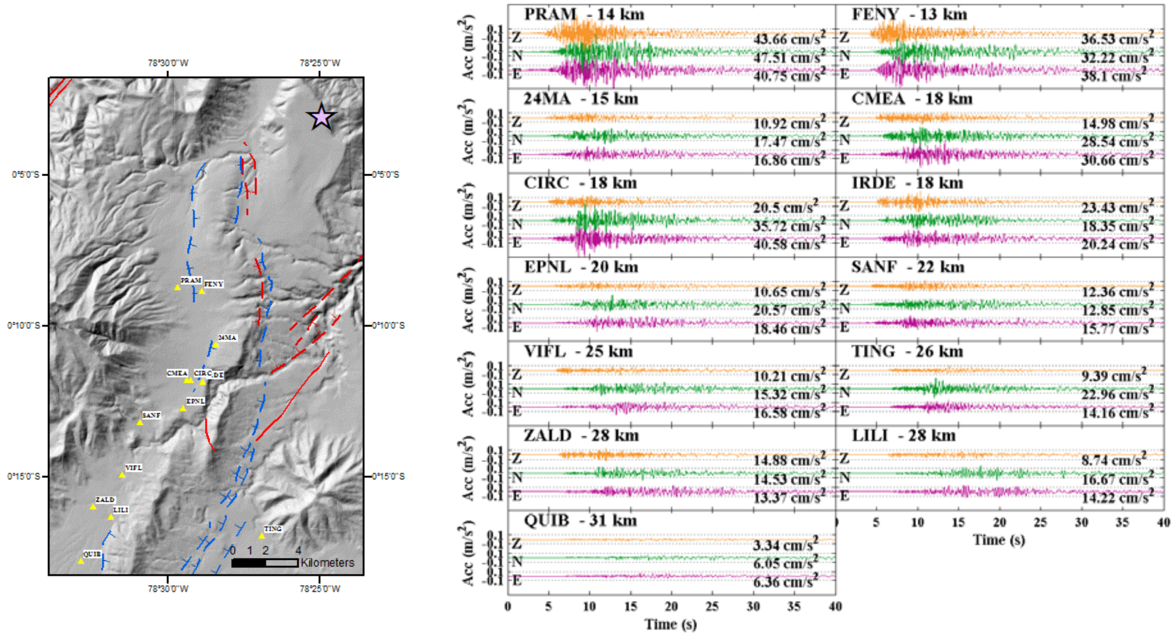

Fig.5: Example of records from RENAC-QUITO from the 20140812195758 earthquake (purple star) with a magnitude of 5.1, depth of 5.3 km and a reverse mechanism. The starting time (0 s) corresponds to the time when the events occurred. The same scale is used to observe the attenuation of the signals with the distance.

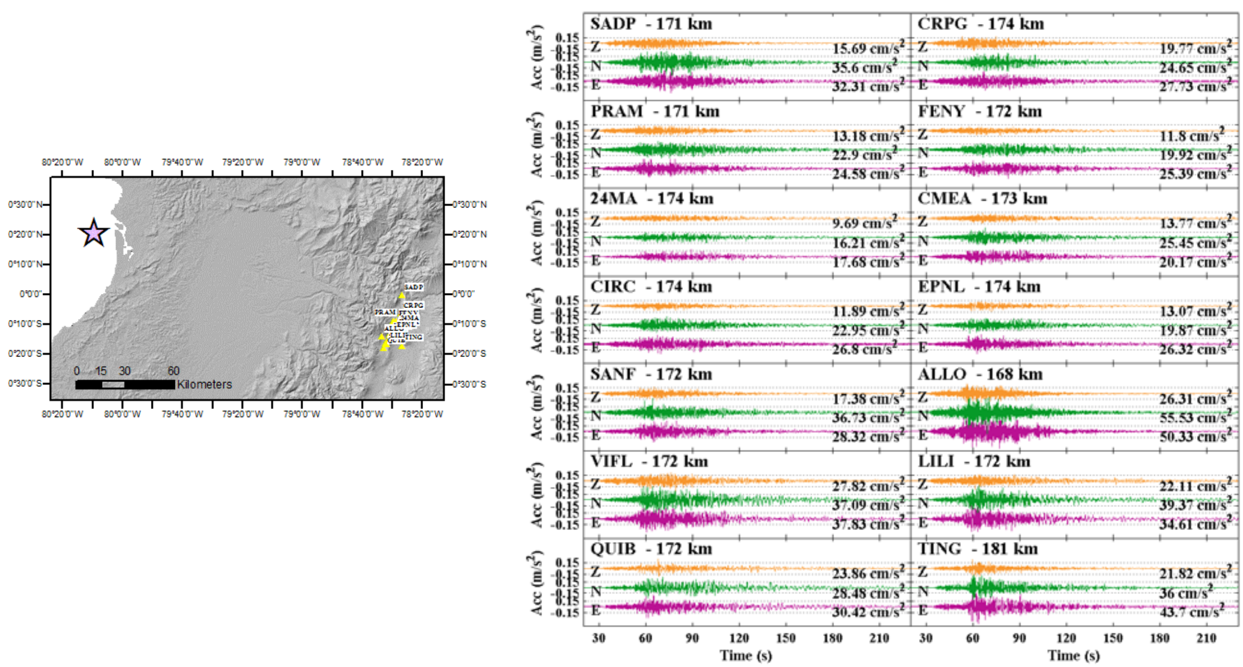

Fig. 6: Example of records from RENAC-QUITO from the 20160416235833 earthquake (purple star) with a Mw of 7.8 (USGS), depth of 17 km and a reverse mechanism. The starting time (0 s) corresponds to the time when the events occurred. The same vertical scale is used.

4.1 HVSR using ambient noise (mHVSR)

This method has been applied by Alfonso-Naya et al. (2012) [3] for 16 sites of RENAC-QUITO (Fig. 7). They followed the SESAME (2004) project [18] specifications to perform the field measurements. The ambient noise was measured with a seismometer Lennartz LE-3D/5s and with a digitizer Reftek RT-130. The recording times vary from 30 minutes to an hour. The open-source Geopsy software was used to process the data (www.geopsy.org) with windows of 40 s and the Konno and Ohmachi (1998) [19] smoothing bandwidth of 40.

4.2 HVSR using earthquake recordings [eHVSR]

The IGEPN and ISC catalogs were employed to search events recorded by RENAC-QUITO between 01-10-2009 and 30-04-2016. From the simple Kanno et al. (2006) ground motion prediction equation [20], 194 events were identified with predicted peak ground acceleration [PGA] larger than 10 cm/s^2. To obtain preliminary results, the time series windowing was applied automatically. The noise window corresponds to 60 s window defined 1 s before the theoretical P wave time arrival [Tp]. Using the Ktenidou et al. (2014) [21] approach, the signal duration (D_S) is defined with respect to the source and propagation terms, with a minimum duration of 10 s. Thus, the signal window is defined from Tp and D_S. For each record, the signal-to-noise ratio (SNR) is estimated both for the vertical component and for the 2D complex time-series of the S-wave window of the two orthogonal horizontal time histories following Thompson et al. (2012) [22]. A first-order baseline operator and a simple baseline correction are applied at each window for each component. A 5% cosine taper is applied on each side of the window. At the end of the records, zeros are added in order to have the same length for each window and a length proportional to a power of 2. Fourier amplitude spectrum (FAS) are computed and are smoothed according to the Konno and Ohmachi (1998) [19] smoothing with b=40. Then, FAS are resampled for a 500 logarithmically spaced sample vector between 0.1 and 50 Hz. Then, eHVSR is computed for each event for which SNR > 3 and for the larger continuous frequency band. Finally, the geometrical mean of eHVSR is estimated if there are at least 3 records for each frequency (Fig. 7).

4.3 Results

The results from mHVSR and eHVSR are quite comparable, with differences mainly at low frequency due to the lower resolution for mHVSR (Fig. 7). The stations implemented in the southern part of Quito show two well-defined resonance frequency peaks around 0.3 Hz and 4 Hz (case of LILI, VIFL and ZALD). Gueguen et al. (2000) [2] found two amplified frequency peaks at similar geologic locations in Quito. However, QUIB located also in the southern part of the basin show only one peak of frequency 0.4 Hz. In the case of the northern stations (24MA, CIRC, CMEA, EPNL, FENY, IESS, IRDE, PRAM and SANF), the site response is relatively similar and at higher frequencies (around between 0.4 Hz and 8 Hz), there is broadband amplification around 2-3 of amplitude.

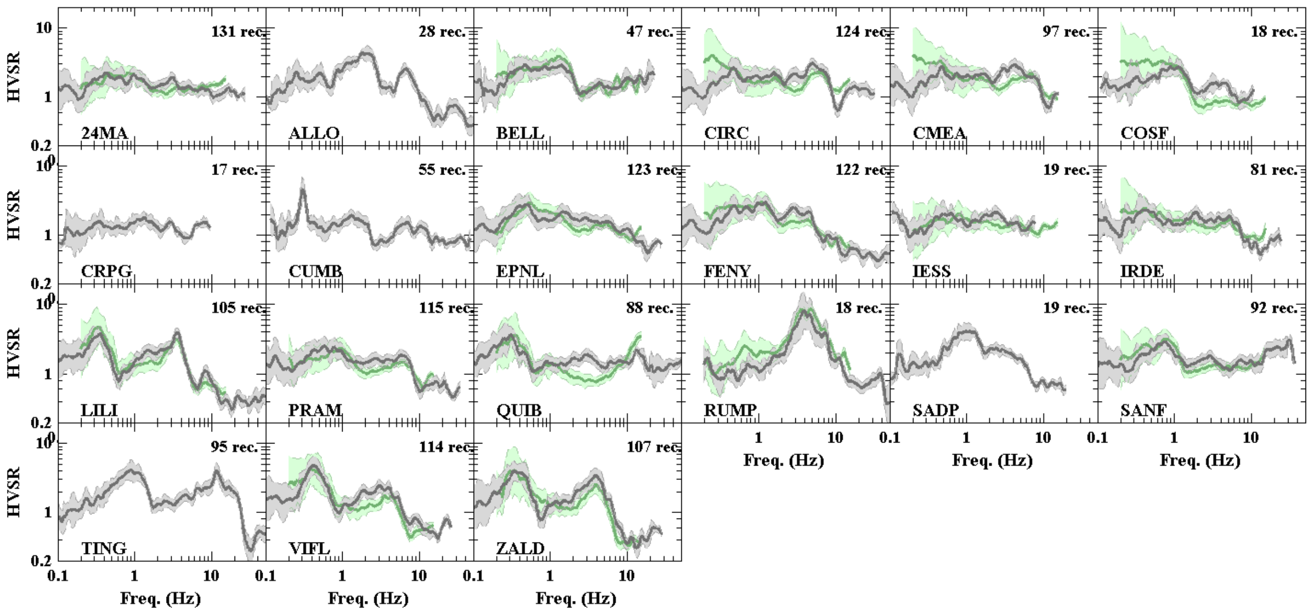

Fig. 7: HVSR results from ambient noise (mHVSR, green) and from accelerometric earthquake recordings (eHVSR, grey). The maximum record numbers used to compute eHVSR are indicated for each site.

5. Basin wave propagation from ambient noise field

Seismic waves generated by earthquakes can be significantly affected by the near-surface velocity structure and its geometry. For example, sedimentary basins can trap and significantly amplify the earthquake ground motion as it has been demonstrated numerically and by dense array observations in Japan and in the U.S. [23, 24, 25, 26]. In addition, such phenomena can be observed even hundreds of kilometers away from the hypocenter, as it was the case for the 1985 Mw 8.0 Michoacán earthquake [27, 28]. Furthermore, the resonance frequency of basins is mainly controlled by the sediment thickness (basin depth), which may vary rapidly in certain areas, producing a strong variability of the ground motion at the surface [29].

Over the last decade, new techniques in seismology have emerged using continuous recordings of the ambient seismic noise field. The seminal work of Shapiro and Campillo (2004) [30] showed that careful processing of the ambient seismic field simultaneously recorded by a pair of stations enables the extraction of the Green's function for the stations. This technique, today referred to as seismic interferometry, has been used to characterize wave amplification in sedimentary basins. Savage et al. (2013) [31] extracted Green's functions between stations located in the Canterbury region of New Zealand and used mHVSR of the first higher-mode Rayleigh waves to determine the basement resonance period. Denolle et al. (2014) [25] studied the wave propagation in the Kanto basin using virtual sources located outside the basin and showed that the basin response is strongly affected by the direction of the incoming seismic wavefield. More recently, Boue et al. (2015) [32] analyzed basin edge effects in the Kanto basin using Green's functions extracted from the Metropolitan Seismic Network (MeSO-net). These studies observed complex mode conversions, reflections, and diffractions, dominate the ground motion in the vicinity of the basin edges.

In this study, we use seismic interferometry through deconvolution proposed by Prieto and Beroza (2008) [33] to obtain the impulse response of the basin situated between two stations. We use one week of continuously recorded seismic ambient noise from the RENAC for the month of January 2015. We compute seismic interferometry between all pair of stations, and the impulse response for the NS components is shown in Fig. 8 for inter-station distances up to 6 km. The synthetized ground motion is filtered between 0.25 and 0.45 Hz. We can observe that stations located in the southern part of the Quito basin present a stronger response with respect to the northern part in this frequency band. Moreover, this preliminary analysis also indicates a directionality of seismic sources. Indeed, impulse responses with respect to station QUIT show stronger amplitude in the non-causal part. Conversely, stations ZALD and VIFL, located more to the north show more energy in the causal part of the interferograms. These observations need to be analyzed with more recording time and also to determine the preferential direction of the seismic response of the basin. This means that we need to know whether the seismic response depends on the direction of the incident wavefield as it has been observed in the Kanto basin in Japan [23]. Finally, our observations suggest that the southern part of the Quito basin may be thicker, which was already suggested by Alfonso-Naya et al. (2013) [3] using HVSR to determine the fundamental resonance frequency in the whole basin.

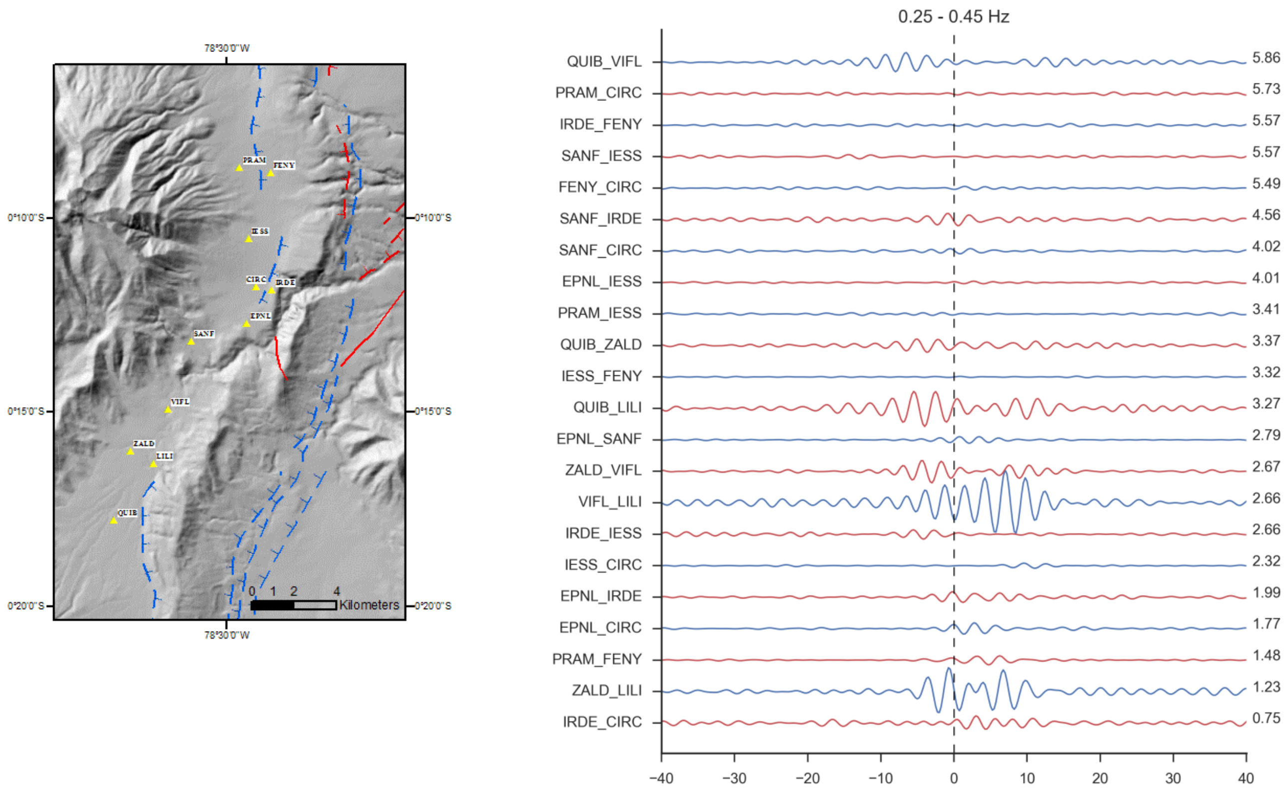

Fig. 8: Inteferograms filtered between 0.25 and 0.45 Hz for the NS components for pair of stations. The first station name is the reference for the seismic interferometry computation. At the right, the inter-station distance in km is indicated.

6. Conclusions

The Red Nacional de Acelerógrafos (RENAC) deployed since 2009, is a high quality accelerometric network in an urban environment. Eighteen stations are in proper working conditions with continuous recordings of ground acceleration at the free surface and provide a sufficient numbers of high quality data to improve the estimations of the potential site effects in Quito.

In this study, the horizontal-to-vertical spectral ratio methods (HVSR) are employed from noise (microseism, mHVSR) and earthquake (eHVSR) records to estimate the site resonant frequency peaks. While these two methods yield comparable results, this study shows that the southern part of Quito has a behavior different of the northern part. The southern part of the basin appears to preferentially amplifies frequencies at around 0.3 Hz and also around 4 Hz. For example, in the case of the Pedernales regional signal, it’s possible to observe longer duration and larger amplitude signals. In addition, the ambient noise recorded by the accelerometers was analyzed by seismic interferometry techniques. Interferograms are higher quality in the southern part than in the northern part of the basin, suggesting a possibly more pronounced site effect in the south due to thickening of the Quito basin in that direction.

7. Acknowledgements

Any opinions, findings, and conclusions or recommendations expressed in this material are those of the authors and do not necessarily reflect the views of the Consortium of Organizations for Strong-Motion Observation Systems (COSMOS) Facilitation Committee for the Development of the COSMOS International Guidelines for the Application of NonInvasive Geophysical Techniques to Characterize Seismic Site Conditions. This contribution is part of an Ecuadorian–French cooperation program between the Instituto Geofisico, Escuela Politécnica Nacional (IG-EPN), Quito, Ecuador; Institut de Recherche pour le Développement (LMI SVAN). This work is supported both by the French project REMAKE (Seismic Risk in Ecuador: Mitigation, Anticipation and Knowledge of Earthquakes); and by the Ecuadorian project SEMPLADES (Generación de capacidades para la difusión de alertas tempranas y para el desarrollo de instrumentos de decisión ante las amenazas sísmicas y volcánicas dirigidos al Sistema nacional de gestión de riesgos). We are also grateful to Victor Alfonso-Naya who initiated this work. The seismic catalog used in this article is available by request from the Red Nacional de Sismografos (RENSIG) at http://www.igepn.edu.ec/solicitud-de-datos.

8. Copyrights

9. References

[1] Beauval C, Yepes H, Bakun WH, Egred J, Alvarado A, Singaucho JC (2010): Locations and magnitudes of historical earthquakes in the Sierra of Ecuador (1587-1996). *Geophysical Journal International*, **181**, 1613–1633.

[2] Gueguen P, Chatelain J-L, Guiller B, Yepes H (2000): An indication of the soil topmost layer response in Quito (Ecuador) using noise H/V spectral ratio. *Soil Dynamics and Earthquake Engineering*, **19(2)**, 127-133.

[3] Alfonso-Naya V, Courboulex F, Bonilla LF, Ruiz M, Vallée M, Yépes H (2012): A large earthquake in Quito (Ecuador): ground motion simulations and site effects. *15th World Conference on Earthquake Engineering, Lisbon, Portugal*, **#4475**, 10 pages.

[4] Nakamura Y. (1989). A method for dynamic characteristics estimations of subsurface using microtremors on the ground surface. *QR of RTRI*, **1;30**:25–33.

[5] Lermo, J. and F.J. Chavez-Garcia, (1993). Site effect evaluation using spectral ratios with only one station, *Bull. Seism. Soc. Am.* **83**, 1574-1594.

[6] Cauzzi, C., & Clinton, J. (2013). A high-and low-noise model for high-quality strong-motion accelerometer stations. *Earthquake Spectra*, *29*(1), 85-102.

[7] Alvarado, A., Audin, L., Nocquet, J. M., Lagreulet, S., Segovia, M., Font, Y., ... & Jarrin, P. (2014). Active tectonics in Quito, Ecuador, assessed by geomorphological studies, GPS data, and crustal seismicity. Tectonics, 33(2), 67-83.

[8] Del Pino I. and Yepes H. (1990). Apuntes para una Historia Sismica de Quito. Centro Histórico de Quito: Problemática y Perspectivas, Sene Quito. I. Municipio de Quito y Junta de Andalucía. Min. de Asuntos Exteriores de España, Quito, pp. 67-100.

[9] Palacios, P., and H. Yepes (2011). Analysis de la magnitud de duracion, Instituto Geofisico, Escuela Politecnica Nacional, Quito, internal report, 18 pp (in Spanish).

[10] Hanka, W., A. Heinloo and K. Jaeckel (2000). Networked Seismographs: GEOFON Real-Time Data Distribution, Orpheus Newsletter, Vol 2(3).

[11] Heinloo, A. and C. Trabant (2003). SeisComP 2.0 Manual, Potsdam.

[12] Beauval, C., Yepes, H., Palacios, P., Segovia, M., Alvarado, A., Font, Y., ... & Vaca, S. (2013). An earthquake catalog for seismic hazard assessment in Ecuador. Bulletin of the Seismological Society of America, 103(2A), 773-786.

[13] Singaucho JC (2014). Evaluación de intensidades sísmicas (Sismo de Calderón 12 de agosto de 2014 14:58 TL) http://www.igepn.edu.ec/IG/Reporte_de_intensidades_12082014_v02.pdf (Last accessed 03/05/2016).

[14] Singaucho JC and Perrault M. (2016). Evaluación de intensidades sismo en Pedernales. http://www.igepn.edu.ec/servicios/noticias/1316-informe-sismico-especial-n-12-2016. (Last accessed 03/05/2016).

[15] Bonilla, L.F., Steidl, Jamison H., Lindley, Grant T., Tumarkin, Alexei G., and Archuleta, Ralph J., (1997). Site amplification in the San Fernando Valley, California; variability of site-effect estimation using the S-wave, coda, and H/V methods, *Bull. Seism. Soc. Am*. **87, 3**, 710-730.

[16] Field, E. H., Clement, A. C., Jacob, K. H., Aharonian, V., Hough, S. E., Friberg, P. A., ... & Abramian, H. A. (1995). Earthquake site-response study in Giumri (formerly Leninakan), Armenia, using ambient noise observations. Bulletin of the Seismological Society of America, 85(1), 349-353.

[17] Kawase, H., Matsushima, S., Satoh, T., & Sánchez-Sesma, F. J. (2015). Applicability of Theoretical Horizontal-to-Vertical Ratio of Microtremors Based on the Diffuse Field Concept to Previously Observed Data. Bulletin of the Seismological Society of America, 105 (6), 3092-3103.

[18] SESAME (2004), Guidelines for the implementation of the H/V spectral ratio technique on ambient vibrations - measurements, processing and interpretations. SESAME European research project, deliverable D23.12.

[19] Konno K., and Ohmachi T (1998). Ground-motion characteristics estimated from spectral ratio between horizontal and vertical components of microtremor. Bulletin of the Seismological Society of America, 88(1):228–241.

[20] Kanno, T., Narita, A., Morikawa, N., Fujiwara, H., & Fukushima, Y. (2006). A new attenuation relation for strong ground motion in Japan based on recorded data. Bulletin of the Seismological Society of America, 96(3), 879-897.

[21] Ktenidou, O., T. Kishida, R. Darragh, W. Silva, and N. Abrahamson (2014), Fourier spectra and kappa0 (κ_0) estimates for rock stations in the nga-west2 project, in Proceedings of the 10th U.S. National Conference on Earthquake Engineering, Frontiers of Earthquake Engineering, Anchorage, Alaska.

[22] Thompson, E. M., L. G. Baise, Y. Tanaka, and R. E. Kayen (2012), A taxonomy of site response complexity, Soil Dynamics and Earthquake Engineering, 41, 32–43.

[23] Koketsu, K., K. Hatayama, T. Furumura, Y. Ikegami, and S. Akiyama (2005). Damaging Long-period Ground Motions from the 2003 Mw 8.3 Tokachi-oki, Japan Earthquake, Seismol. Res. Lett., 76, 67–73, doi:10.1785/gssrl.76.1.67.

[24] Viens, L., K. Koketsu, H. Miyake, S. Sakai, and S. Nakagawa (2016). Basin-scale Green's functions from the ambient seismic field recorded by MeSO-net, Journal Geophysical Research, in press.

[25] Denolle, M. A., H. Miyake, S. Nakagawa, N. Hirata, and G. C. Beroza (2014). Long-period seismic amplification in the Kanto Basin from the ambient seismic field, Geophys. Res. Lett., 41, 2319–2325, doi:10.1002/2014GL059425.

[26] Olsen, K.B., R.J. Archuleta, and J.R. Matarese (1995). Three-dimensional simulation of a magnitude 7.75 earthquake on the San Andreas fault, *Science*, **270**, 1628-1632.

[27] Anderson, J. G., P. Bodin, J. N. Brune, J. Prince, S. K. Singh, R. Quaas, and M. Onate (1986). Strong ground motion from the Michoacán, Mexico, earthquake, Science, 233, 1043–1049, 211 doi:10.1126/science.233.4768.1043.

[28] Beck, J. L., and J. F. Hall (1986). Factors contributing to the catastrophe in Mexico City during the earthquake of September 19, 1985, Geophys. Res. Lett., 13, 593–596, doi: 214 10.1029/GL013i006p00593.

[29] Bonilla, L.F., C. Gélis, and J. Régnier (2011). The challenge of nonlinear site response: field data observations and numerical simulations, *Proceedings of Fourth Conference on the Effects of the Surface Geology on the Ground Motion*, UC Santa Barbara, California.

[30] Shapiro, N. M., & Campillo, M. (2004). Emergence of broadband Rayleigh waves from correlations of the ambient seismic noise. *Geophysical Research Letters*, *31*(7).

[31] Savage, M. K., F.-C. Lin, and J. Townend (2013). Ambient noise cross-correlation observations of fundamental and higher-mode Rayleigh wave propagation governed by basement resonance, Geophys. Res. Lett., 40, 3556–3561, doi:10.1002/grl.50678.

[32] Boue, P., M. A. Denolle, N. Hirata, S. Nakagawa, and G. C. Beroza (2015). Beyond Resonance: Characterizing Complex Basin Effects Using a Dense Seismic Array, Abstract S24B-08, presented at 2015 Fall Meeting, AGU, San Francisco, Calif., 14-18 dec.

[33] Prieto, G. A., and G. C. Beroza (2008). Earthquake ground motion prediction using the ambient seismic field, Geophys. Res. Lett., 35, L14304, doi:10.1029/2008GL034428.